The hypoglycemic potential of genus *Morus*: Bioavailability and molecular docking between secondary metabolites of *Morus alba* L. and sulfonylurea receptor 1 (SUR1)

Potencial hipoglicémico del género *Morus*: biodisponibilidad y docking molecular entre metabolitos secundarios de *Morus alba* L. y el receptor de sulfonilurea (SUR1)

Emildo Marcano[1,*], Ysbelia Sánchez[2]

Abstract

It is reported the bioavailability analysis for ten secondary metabolites with hypoglycemic activity from *Morus alba* L. Additionally, the molecular similarity analysis of each metabolite is presented and compared with nateglinide, nepaglinide, and other hypoglycemic molecules referents. The mode of interaction through molecular docking between each secondary metabolite and the zone of action for repaglinide (RPG) in the sulphonylurea receptor 1 (SUR1) is also presented. The molecular geometry for structures was optimized with HF/6-31+G (d,p) level and functional density methods at the CAM-B3LYP/6-31+G (d,p) level. The bioavailability and molecular docking calculations were performed using the algorithms incorporated in the chemo informatic servers and AutoDock Vina. The results show that the structures studied lead a good permeability through the cell membrane, by complying with Lipinski's "rule of 5"; namely: log P<5, molecular weight <500, acceptor sites for hydrogen bonds <10, donor sites for hydrogen bonds <5 and a molecular volume <500. The molecular similarity was evaluated by averaging geometric parameters (3D-Shape) and electrostatic potential (ESP). The results show that most secondary metabolites would have a similar mode of action as the neteglinide, with the average similarity between 0.72 and 0.80. This last idea is reinforced by the results for molecular docking with the nepaglinide active site of SUR1, highlighting the interaction of the molecules studied with the amino acid residues: Arg-1246, Tyr-377, Asn-437, Leu-434, Phe-433, Trp-430, and Ile-381, with arranging interaction-free energy between -5.2 and -7.9 Kcal/mol.

Key words: SUR1, metabolites, *Morus alba* L., hypoglycemic, diabetes.

Resumen

Se reporta el análisis de biodisponibilidad para diez metabolitos secundarios con actividad hipoglucémica para *Morus alba* L. Adicionalmente, se presenta el análisis de similaridad molecular de cada metabolito contra nateglinida, repaglinida y otras moléculas de referencia. También se presenta el modo de interacción a través del docking molecular entre cada metabolito secundario y la zona de acción de repaglinida (RPG) en el receptor de sulfonilurea (SUR1). La geometría molecular de las estructuras se optimizó con métodos de nivel HF/6-31+G (d, p) y CAM-B3LYP / 6-31+G (d, p). Los cálculos de biodisponibilidad y docking molecular se realizaron utilizando los algoritmos incorporados en los servidores de quimio-informática y autodock vina. Los resultados muestran que las estructuras estudiadas presentan una buena permeabilidad a través de la membrana celular, cumpliendo con la "regla de 5" de Lipinski; a saber: Logp <5, masa molecular <500, sitios aceptores para enlaces de hidrógeno <10, sitios donantes para enlaces de hidrógeno <5 y un volumen molecular <500. La similaridad molecular se evaluó promediando parámetros geométricos (3D-Shape) y potencial electrostático (ESP). Esta última idea se ve reforzada por los resultados de docking molecular con el sitio activo de repaglinida para SUR1, destacando la interacción de las moléculas estudiadas con los residuos de aminoácidos: Arg-1246, Tyr-377, Asn-437, Leu-434, Phe-433, Trp-430 e Ile-381, con un rango de energía libre de interacción entre -5,2 y -7,9 kcal/mol.

Palabras clave: SUR1, metabolitos, *Morus alba* L., hipoglicemiantes, diabetes.

[1] Departamento de Química. Laboratorio de Computación de Alto Rendimiento. Universidad Nacional Experimental del Táchira (UNET), Venezuela.
[2] Laboratorio de Investigaciones Genéticas. Universidad Nacional Experimental del Táchira (UNET), Venezuela.
* Correspondence: jedi148@gmail.com

Introduction

Diabetes is a chronic disease that features abnormal glucose homeostasis. About 10% of patients have Type 1 diabetes and 90% have Type 2 diabetes. Type 1 diabetic patients require insulin treatment for survival because of an absolute insulin deficiency. Type 2 diabetic patients are usually treated by a combination of diet and exercise, or with pharmacological agents (such as sulphonylureas, biguanides, and thiazolidinediones) and insulin to control hyperglycemia caused by an increase of insulin resistance, impaired pancreatic insulin secretion, and/or increased hepatic glucose production (Henquin, 2004). It is known that when the concentration of glucose increases, β-cell metabolism accelerates, leading to the closure of K_{ATP} channels in the plasma membrane. These channels are composed of the pore-forming Kir6.2 (inward-rectifying potassium channel 6.2) and the regulatory sulphonylurea receptor 1 (SUR1). The binding of intracellular ATP to Kir6.2 closes the channel, whereas binding of MgADP to SUR1 opens the channel. The increase in the ATP/ADP ratio resulting from the metabolism of glucose thus closes the channel. The consequence is a depolarization of the plasma membrane, with the opening of voltage-dependent Ca^{2+} channels, acceleration of Ca^{2+} influx, and an increase in the concentration of cytosolic free Ca^{2+} ([Ca2+]) that is necessary and sufficient to trigger insulin secretion (Proks and Ashcroft, 2009). In the past decade has been shown that several drugs can be interacting with the SUR1 to driven insulin secretion (Shinkai, 2000). Therefore, sulphonylurea insulin secretagogues as glibenclamide and non-sulphonylurea as nateglinide and repaglinide exerts an insulinotropic effect, by the blockade of KATP channels in pancreatic β-cells (Hansen *et al.*, 2002). Recently, three structures of pancreatic K_{ATP} channels solved by cryo-electron microscopy have been reported (Wu *et al.*, 2018). These structures depict the binding site of the antidiabetic drug glibenclamide, indicate how Kir6.2 N-terminus participates in the coupling between the peripheral SUR1 subunit and the central Kir6.2 channel, reveal the binding mode of activating nucleotides and suggest the mechanism of how Mg-ADP binding on nucleotide-binding domains drives a conformational change of the SUR1 subunit. Equally, the binding site of the antidiabetic drug repaglinide (RPG) in the SUR1 subunit has been reported (Ding *et al.*, 2019). However, despite widely used, these drugs shave varying cross-reactivity with related channels in extrapancreatic tissues such as heart, vascular smooth, and skeletal muscle (Gribble and Reimann, 2003). As newer oral diabetes agents continue to emerge on the market, comparative evidence is required to guide appropriate therapy. Therefore, the quest for new and major antidiabetics compounds follows been a challenge. In this framework, several plants have been used for the treatment and management of diabetes in ethnomedicine, ranked in order of most widely cited includes *Momordica charantia* L., *Catharanthus roseus* (L.) G. Don, *Syzygium cumini* (L.) Skeels, *Trigonella foenum-graecum* L., *Phyllanthus emblica* L., *Phyllanthus niruri* L., and *Morus alba* L. (Marles and Farnsworth, 1995). Specifically, the genus *Morus* in the Moraceae family is globally distributed under varied climatic conditions, ranging from tropical to temperate. This genus contains 24 species and one subspecies and *Morus*

alba L. is a dominant species among them (Yuan and Zhao, 2017). In the past decade, many secondary metabolites of *M. alba* as caffeic acid (Matboli *et al.*, 2017), gallic acid (Doan *et al.*, 2015), cinnamic acid (Adisakwattana, 2017), chlorogenic acid (Meng *et al.*, 2013) and others have been investigated as possible antidiabetics compounds (Vinayagam *et al.*, 2015). Most of the reported research on the antidiabetic behavior of these secondary metabolites has been directed towards experimental results, and few reports are available on molecular vision and the location of molecular targets that explain their possible action. Therefore, in this work, we present a theoretical study of bioavailability and molecular recognition between secondary metabolites of *M. alba* and SUR1. Our contribution focuses on five aspects: I) the prediction of the bioavailability of the structures of interest, based on the Lipinski parameters ("rule of five"); II) the exploration of the molecular similarity using as references the structures of nateglinide and repaglinide, from the calculation of 3D-shape and electrostatic potential (ESP); III) prediction of bioactivity scores using bioinformatics tools, IV) molecular docking of the interest structures and the binding site of repaglinide in the SUR1 protein, V) normal mode analysis (NMA) for the structure with the major interaction mode into the SUR1. With our results, we hope to give molecular insight into the use of secondary metabolites of *M. alba* in the potential or possible treatment of diabetes mellitus.

Computational details

Geometric optimization and molecular similarity analysis

The molecular similarity principle states that molecules with similar structures tend to have similar properties. Indeed, the observation that common substructural fragments lead to similar biological activities, can be quantified from database analysis (Bender and Glen, 2004; Eckert and Bajorath, 2007). In this paper, we have chosen ten secondary metabolites with hypoglycemic activities reported in *M. alba* for the similarity analysis, using as references the structures of nateglinide and repaglinide, which are known for their interaction with SUR1 (**Figure 1**). For all structures, the geometric optimizations were carried out at HF/6-31+G

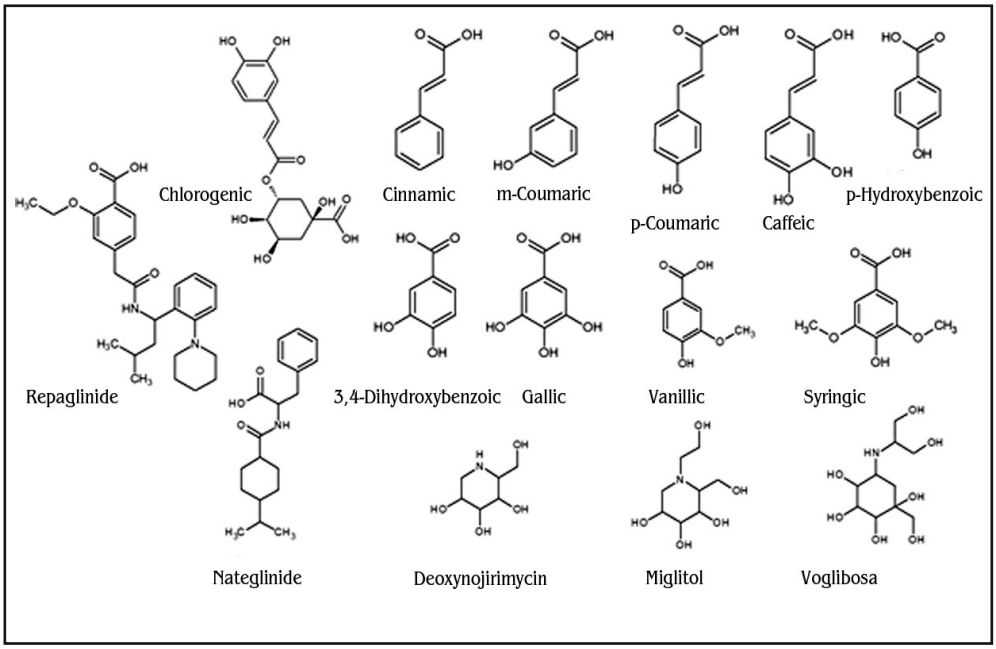

Figure 1. Reference molecules and secondary metabolites (acids) of *M. alba* ligands studied.

(d,p) level using the GAMESS software package (Schmidt *et al.*, 1993). The electronic correlation was account for CAM-B3LYP/6-31+G (d,p) level. The molecular similarity calculations were carried out with the ShaEP software package. ShaEP performs a rigid-body superimposition of 3D molecular models, using a matching algorithm (Vainio *et al.*, 2009). Two characteristic scores were calculated for comparison: 3D shape and electrostatic potential (ESP) (Shin *et al.*, 2015). These scores range is from 0 to 1, in which 0 and 1 correspond to no similarity and the same molecules, respectively.

Bioavailability and bioactivity score prediction

Properties of molecules such as bioavailability or membrane permeability have often been connected to simple molecular descriptors such as logP (partition coefficient), molecular weight (MW), or counts of hydrogen bond acceptors and donors in the molecule (Muegge, 2003). These descriptors are included in the named Lipinski "Rule of Five" (Lipinski *et al.*, 1997). The rule states that most molecules with good membrane permeability have logP ≤ 5, molecular weight ≤ 500, number of hydrogen bond acceptors ≤ 10, and number of hydrogen bond donors ≤ 5. To evaluate the bioavailability of the secondary metabolites studied, Lipinski´s parameters were calculated and compared with those in nateglinide and repaglinide molecules. Equally, the predicted bioactivity scores of studied compounds as well as their comparison with the standard drugs (1-deoxynojirimycin, miglitol, and voglibose) for GPCR ligand, ion channel modulator, a kinase inhibitor, nuclear receptor ligand, protease inhibitor, and enzyme inhibitory activity were evaluated. These calculations were carried out using Molinspiration Cheminformatics software (Molinspiration, 1986).

Preparation of SUR1, molecular docking, and normal mode analysis

Cryo-electron microscopy structure of the pancreatic KATP channel in complex with inhibitory RPGAndadenosine-5'-(γ-thio)-triphosphate (ATPγS) (PDB ID: 6JB3) at 3.3 Å of the resolution was used for studying the interaction between the secondary metabolites of *M. alba* (**Figure 1**) and SUR1 (Ding *et al.*, 2019). From PDB structure we retained an RPG-SUR1 complex consisting of only B chain (1582 residues, from *VAL*-215 to *TYR*-1326). Hydrogen atoms were added to the model using the VEGA ZZ package (Pedretti *et al.*, 2004). Atomic charges were assigned using the Gasteiger-Marsili method (Gasteiger and Marsili, 1980). RPG and other crystal molecules were removed. Secondary metabolites of *M. alba* ligands were optimized using CAMB3LYP/6-31+G (*d,p*) level using the GAMESS software package. Later, the ligands were prepared for docking experiments defining rotatable bonds using AutoDock Tools version 1.5.6. A grid box size of 20.25, 20.25, 20.25 Å was generated and allocated at the center of the receptor-binding site using x, y, and z coordinates of 156.89, 103.9 and 157.19. Molecular docking simulations and visualization of all structures were performed using AutoDockVina software. Co-crystallized ligands were re-docked as validation of the docking protocol. Finally, for the molecule with the major performance (bioavailability and molecular docking) have used the default settings of WEBnm@ server to performance an Atomic Displacement Analysis, to identify the flexible region of the SUR1, and Mode Visualization and

Vector Field Analysis to obtain the direction of collective motions of the SUR1 (Hollup *et al.*, 2005).

Results and discussion

Lipinski's parameters

Lipinski's rule is widely used to determine molecular properties that are important for a drug's pharmacokinetics in vivo. **Table I** contains the calculated percentage of absorption (%ABS), molecular polar surface area (TPSA), and Lipinski parameters of the *M. alba* secondary metabolites investigated. Molecular hydrophobicity or lipophilicity is indicated by the octanol/water partition coefficient (Log P). The hydrophilic/lipophilic nature of drug molecules affects drug permeability across the cell membrane. Log P values of all the secondary metabolites studied were found to be lower than 5, in agreement with Lipinski's rule of five. Chlorogenic acid presents the lowest Log P (-0.45), indicating that this metabolite has a hydrophilic character, suggesting poor permeability across the cell membrane. However, chlorogenic acid has been reported for its hypoglycemic effect (Nicasio *et al.*, 2005). The rest of the metabolites studied have Log P values between 0.59 and 1.91, indicating greater lipophilicity and therefore better permeability through the cell membrane. In fact, cinnamic acid presents a Log P-value that is in the known range for many hypoglycemic drugs (Remko, 2009) and it has been reported for its antidiabetic activity (Vinayagam *et al.*, 2015). p-hydroxy-benzoic acid and p-coumaric acid have a Log P range for a drug with good oral and intestinal absorption (1.35-1.8) (Bhal, 2012).

Table I

Calculated percentage of absorption (%ABS), molecular polar surface area (TPSA), and Lipinski parameters of the *M. alba* secondary metabolites investigated

Molecule (Acid)	%ABS	Volume	TPSA	Nrot	n ON acceptors	n OHNH donors	Log P	MW
Chlorogenic	52.2	296.97	164.74	5	9	6	-0,45	354.31
p-Hydroxybenzoic	89.6	119.06	57.53	1	3	2	1.37	138.12
Vanillic	86.0	144.61	66.76	2	4	2	1.19	168.15
Cinnamic	96.1	138.46	37.30	2	2	1	1.91	148.16
Caffeic	82.2	154.50	77.75	2	4	3	0.94	180.16
Gallic	75.2	135.10	97.98	1	5	4	0.59	170.12
p-Coumaric	89.2	146.48	57.53	2	3	2	1.43	164.16
m-Coumaric	89.2	146.48	57.53	2	3	2	1.41	164.16
Syringic	82.8	170.15	76.00	3	5	2	1.20	198.17
3,4-Dihydroxybenzoic	82.2	127.08	77.75	1	4	3	0.88	154.12
Miglitol	72.9	189.18	104.38	3	6	5	-2.79	207.23
Voglibose	56.0	238.17	153.62	5	8	8	-3.98	267.28
Deoxynojirimycin	76.9	147.18	92.94	1	5	5	-2.40	163.17
Nateglinide	86.9	316.03	66.40	6	4	2	2.56	317.43
Rapaglinide	81.8	442.52	78.87	10	6	2	4.87	452.60

Total polar surface area (TPSA) is closely related to the hydrogen bonding potential of a molecule and is a good predictor of drug transport properties such as intestinal absorption, bioavailability, blood-brain barrier penetration, etc. Molecules with a polar surface area of greater than 140 Å^2 tend to be poor at permeating cell membranes (Pajouhesh and Lenz, 2005). For molecules to penetrate the blood-brain barrier a PSA less than 90 Å^2 is usually needed

(Hitchcock and Pennington, 2006). TPSA of molecules secondary metabolites was found in the range of 37-164 Å^2, which in agreement with the limits mentioned above. Likewise, these values are comparable to those exposed by know hypoglycemic drugs (Remko, 2009) and to those exposed by other secondary metabolites in other plants (Hossain *et al.*, 2016). The number of rotatable bonds is a simple topological parameter that measures molecular flexibility and is considered to be a good descriptor of the oral bioavailability of drugs. It has been shown that higher oral bioavailability is associated with a lower rotatable bond count. Rotational bonds make the compounds flexible; hence easily interact with a specific rigid binding area (Veber*et al.*, 2002). All the structures studied show low molecular flexibility due to low rotatable bonds, except chlorogenic acid, which has 5 rotatable bonds. The number of hydrogen bond acceptors (O and N atoms) and the number of hydrogen bond donors (NH and OH) in the tested compounds were found to be within Lipinski's limit i.e. less than 10 and 5 respectively, except chlorogenic acid, whose values are on the limit of the rule. The percentages of absorption for title compounds calculated from TPSA ranged between 52.2 and 96.1% and indicated good oral bioavailability. In fact, when the BOILED-Egg model (Daina and Zoete, 2016) was applied through the Swiss ADME server (Daina *et al.*, 2017), we found a good permeation blood-brain barrier (BBB) probability in the following order: cinnamic acid > p-coumaric acid > p-hydroxybenzoic acid > vanillic acid; and good human intestinal absorption (HIA) probability in the following order: syringic acid > caffeic acid > 3,4-hydroxybenzoic acid > gallic acid > chlorogenic acid.

Bioactivity score

The predicted bioactivity scores of studied compounds, as well as their comparison with the standard drugs (1-deoxynojirimycin, miglitol, and voglibose) for GPCR ligand, ion channel modulator, a kinase inhibitor, nuclear receptor ligand, protease inhibitor, and enzyme inhibitory activity, are summarized in **Table II**. As a general rule, the larger is the bioactivity score, the higher is the probability that the investigated compound will be active. Therefore, a molecule having a bioactivity score of more than 0.00 is most likely to possess considerable biological activities, while values -0.50 to 0.00 are expected to be moderately active and if the score is less than -0.50 it is presumed to be inactive (Ochieng, *et al.*, 2017). **Table II** shows that the secondary metabolites studied can act primarily as ionic channel modulators, nuclear receptor ligands, and other enzyme inhibitors.

Table II
Predicted bioactivity scores of the *M. alba* secondary metabolites investigated

Molecule (Acid)	GPCR ligand	Ion channel modulator	Kinase inhibitor	Nuclear receptor ligand	Protease inhibitor	Enzyme inhibitor
Chlorogenic	0.29	0.14	0.00	0.74	0.27	0.62
p-Hydroxybenzoic	-0.98	-0.39	-1.21	-0.62	-1.19	-0.41
Vanillic	-0.85	-0.42	-0.99	-0.61	-1.12	-0.35
Cinnamic	-0.74	-0.40	-1.14	-0.47	-0.98	-0.30
Caffeic	-0.48	-0.23	-0.81	-0.10	-0.79	-0.09
Gallic	-0.77	-0.26	-0.88	-0.52	-0.94	-0.17
p-Coumaric	-0.56	-0.26	-0.91	-0.12	-0.87	-0.15
m-Coumaric	-0.57	-0.28	-0.94	-0.11	-0.89	-0.16
Syringic	-0.65	-0.28	-0.69	-0.44	-0.82	-0.15
3,4-Dihydroxybenzoic	-0.88	-0.35	-1.10	-0.58	-1.09	-0.34
Miglitol	-0.41	-0.10	-0.53	-0.82	0.11	0.36
Voglibose	0.14	0.16	0.10	0.09	0.34	0.85
1-Deoxynojirimycin	-0.71	-0.25	-0.85	-1.14	0.13	0.29
Rapaglinide	0.14	-0.03	-0.33	0.03	0.07	-0.09
Nateglinide	0.34	0.12	-0.30	0.08	0.59	0.16

Chlorogenic acid also will produce physiological actions by interacting with GPCR ligands and protease inhibitors. In fact, the roles and applications of chlorogenic acid, particularly in relation to glucose and lipid metabolism, have been highlighted (Meng *et al.*, 2013). The only compounds with a moderate bioactivity score for GPCR ligand are the caffeic acid (-0.48), which is comparable with miglitol (-0.41). Caffeic, gallic, coumaric, and syringic acids show an ion channel modulator score com-parable with 1-deoxynojirimycin (-0.25). Equally, these acids present a good nuclear receptor ligand score comparable with miglitol. Also, **Table II** shows the tendencies about the moderated biology activity of the secondary metabolites studies as an enzyme inhibitor, with score values between -0.41and -0.09. This tendency is in agreement with the report for different enzyme's molecular targets, *i.e.,* caffeic acid (Fernandes *et al.*, 2015), gallic acid (Kyriakis *et al.*, 2015), coumaric acid (Shukla *et al.*, 2015).

Molecular similarity

The aim of this paper is the exploration of the antidiabetic potential of the secondary metabolites of *M. alba* (**Figure 1**), through the interaction with different molecular targets. The combination of the literature review and the search for similar structures related to *M. alba* secondary metabolites in the PubChem and DrugBank databases, allowed us to choose two antidiabetic family compounds of interest: Non-sulphonylurea insulin secretagogues (NSIS) and α-glucosidase inhibitors (IAG). Both compound groups have been tested in the past decades (Guardado-Mendoza *et al.*, 2013; Chaudhury *et al.*, 2017; Teng and Chen, 2017). Nateglinide was chosen as non-sulphonylurea insulin secretagogues (Furman, 2017). Also, the secondary metabolites of *M. alba* were studied against three of the well-known IAG such as 1-deoxynojirimycin, miglitol, and voglibose (Ernawati *et al.*, 2018). The mechanisms of actions of these drugs are clarified and all the targets are validated. Moreover, the structural information of the targets is available from the Protein Data Bank. Starting from the knowledge of four molecules identified as antidiabetic drugs we analyzed the molecular similarity between secondary metabolites of *M. alba* and these known drugs to propose the possible antidiabetic action of these structures. Two important properties, 3D-shape, and electrostatic potential (ESP) of secondary metabolites were compared to those of four drugs and the results are shown in **Table III**. It is shown that secondary metabolites studied have a high shape similarity with miglitol and 1-Deoxynojirimycin, with average values of 0.773 and 0.803, respectively. These molecules possess a similar framework of rings, mainly substituted by -OH groups. It is also shown that the four reference drugs have a moderate deep similarity with the most secondary metabolites studied, with average values of 0.494 (<0.600). However, cinnamic acid, m-coumaric acid, and 3,4-dihydroxybenzoic acid have a relatively high ESP similarity (over 0.65) with the Nateglidine.

The high ESP similarity in these compounds may be due to the existence of a plentiful electron-withdrawing functional group close to the molecular ring framework, which is similar to that of nateglidine. In fact, the value of ESP similarity (0.810) between cinnamic acid and nateglidine is due to the highest

Table III
3D-shape and electrostatic potential (ESP) of the *M. alba* secondary metabolites investigated

Molecule (Acid)	Miglitol		Voglibose		Deoxynojirimycin		Nateglinide	
	3D-shape	*ESP*	*3D-shape*	*ESP*	*3D-shape*	*ESP*	*3D-shape*	*ESP*
Chlorogenic	0.803	0.547	0.612	0.469	0.842	0.459	0.594	0.599
p-Hydroxybenzoic	0.777	0.477	0.700	0.458	0.808	0.561	0.601	0.493
Vanillic	0.569	0.400	0.698	0.461	0.594	0.471	0.744	0.481
Cinnamic	0.762	0.495	0.686	0.402	0.818	0.492	0.551	0.810
Caffeic	0.827	0.524	0.699	0.393	0.842	0.476	0.592	0.554
Gallic	0.759	0.449	0.635	0.436	0.765	0.448	0.644	0.554
p-Coumaric	0.757	0.427	0.694	0.405	0.798	0.444	0.642	0.572
m-Coumaric	0.796	0.505	0.675	0.416	0.914	0.534	0.589	0.631
Syringic	0.831	0.476	0.713	0.433	0.796	0.436	0.540	0.524
3.4-Dihydroxybenzoic	0.855	0.487	0.673	0.462	0.851	0.437	0.470	0.650

because of the negatively charged -COOH group and the presence of an aromatic ring nateglidineis an oral antihyperglycemic agent used for the treatment of non-insulin-dependent diabetes mellitus (NIDDM). It belongs to the meglitinide class of short-acting insulin secretagogues, which act by binding to β-cells of the pancreas to stimulate insulin release (Wishart *et al.*, 2017). Specifically, nateglinide exerts an insulinotropic effect, like that of sulphonylureas, by the blockade of K_{ATP} channels in pancreatic β-cells. This blockade decreases K^+ efflux and causes depolarization of the cell membrane, thus opening a voltage-dependent Ca^{2+} channel and allowing extracellular Ca^{2+} to enter the cell. The increase of cytosolic Ca^{2+} in β-cell triggers the movement of insulin granules to the membrane and increases the exocytosis of insulin (Shinkai, 2000). The molecular similarity of cinnamic acid, m-coumaric acid, and 3,4-dihydroxybenzoic acid with nateglidine, suggests that these acids could also interact with SUR1 (**Figure 1**).

Molecular docking

The aim of this paper is the exploration of the antidiabetic potential of the secondary metabolites of *M. alba*, through the interaction with some molecular targets. As an observer in **Table II**, the molecular similarity of cinnamic acid, m-coumaric acid, and 3,4-Dihydroxybenzoic acid with nateglidine, suggests that these acids could also interact with the sulphonylurea receptor (SUR1). Therefore, in the present study, molecular docking was performed to identify the docking score of ten structures of **Figure 1** towards a medium-resolution structure of repaglinide (RPG)-bound mini SUR1 protein recently reported (Ding *et al.*, 2019). Likely nateglidine, repaglinide (RPG) is another short-acting insulin secretagogue widely prescribed for the treatment of type 2 diabetes.

Table IV and **Figure 2** show the RPG binding site in SUR1from Protein Data Bank (PDB: 6JB3). Residues *LEU*-592, *VAL*-596, *TRP*-430, *LEU*-434, *TYR*-377,

Table IV
Binding site and ligand binding energy (LBE, Kcal/mol) for RPG and the secondary metabolites studied in SUR1

Molecule	Glu-1249	Arg-1246	Arg-1300	Asn-1245	Thr-1242	Ser-1238	Arg-306	Tyr-377	Asn-437	Leu-434	Phe-433	Trp-430	Ile-381	Met-441	Leu-592	Val-596
Rapaglidine	x	x	x	x	x	x	x	x	x	x	x	x	x	x	x	x
Chlorogenic acid	x	x	x					x	x	x	x					
p-Hydroxybenzoic acid		x						x	x				x			
Vanillic acid		x						x	x	x	x		x			
Cinnamic acid		x		x		x		x	x	x	x	x	x			
Caffeic acid		x		x	x	x		x			x	x	x			
Gallic acid		x						x	x	x	x		x			
p-Coumaric acid		x	x	x				x	x	x	x	x	x			
m-Coumaric acid		x						x	x	x	x		x			
Syringic acid	x	x	x					x	x		x				x	
3,4-Dihydroxybenzoic acid	x	x	x					x			x		x			

and *ILE*-381 form a pocket to accommodate the hydrophobic region of RPG, and two major polar interactions further aid in its positioning. Residues *ASN*-1245 and *ARG*-1246 coordinate the negatively charged carboxyl group of RPG, whereas *ASN*-437 interacts with the amide linker of RPG.

As observed in **Table IV**, all structures interacting with two main zones according to the RPG binding site. Cinnamic acid, p-coumaric, m-coumeric, and caffeic interacting with *Arg*-1246 residue (**Figure 3**) with a binding energy average of -5.8 Kcal/mol, 27% less than repaglinide. Specifically, the carboxyl group in the cinnamic acid interacting across a hydrogen bond with both, *Arg*-1246 (2.14 Å) and *Asn*-1245 (2.56 Å), with values of Hyd from -3.04 to -2.97 (**Figure 3**). In both cases, the π–π interaction with *Tyr*-377 residue also is observed.

The substitution of the -OH group in m-coumaric acid lead to an interaction mode aligned with the *Tyr*-377. In this case, a hydrogen bond between *Tyr*-377(-OH):---(COOH) m-coumaric (2.58 Å) and a π–π interaction is founded. π–π interaction with *Tyr*-377 also is founded for caffeic acid, and two hydrogen bonds (1.89 Å and 1.95 Å) are observed when a second -OH group is substituted. All cinnamic acid derivates interact with almost hydrophobic regions in SUR1 (**Table IV**). However, as observed in **Figure 3**, m-coumaric and caffeic acid lead to a major hydrophobic interaction (Hyd-I), evaluated by Fermi's equation (-2.60 and -2.58, respectively). These values could be a relationship with the π–π interaction. Hydroxybenzoic acid derivates (p-hydroxybenzoic acid, 3,4-hydroxybenzoic acid, and gallic acid) also interacting with the hydrophobic region.

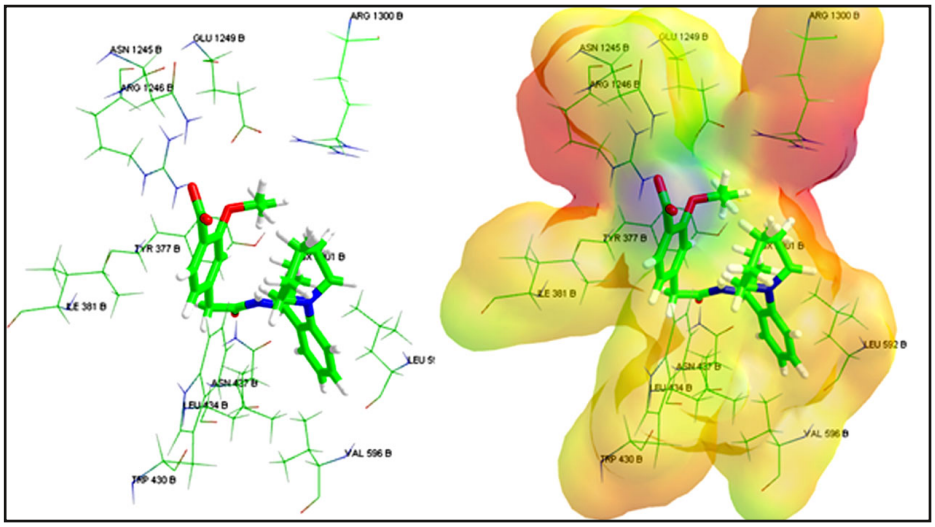

Figure 2. RPG (PDB: 6JB3) binding site in SUR1 and potential electrostatic map (MEP)

As showed in **Figure 4**, π–π interaction with *Tyr*-377 residue also is observed, and additionally, gallic acid showed a hydrogen bond (2.41 Å) with the *Phe*-433 residue. The addition of hydroxyl groups slightly increases the value of hydrophobic interactions (-2.59 → -2.97); however, when a methoxy group is editioned (Vanillic acid), these interactions decrease significantly up to -0.76. Two hydrogen bonds (2.16 Å and 2.12 Å) are observed for the vanillic acid and *Asn*-437/*Arg*-1246 residues.

Cinnamic and p-hydroxybenzoic acids derivate of **Figure 1** and **Table I** showed a binding energy average value of -5.8 Kcal/mol, 27% less than repaglinide, the reference ligand reported for SUR1 (Ding *et al.*, 2019) using in this work. However, several references reporting the use of these molecules for the management of NIDDM. For example, the gallic acid present in the fruit rind of *Terminalia bellerica* Roxb. has been reported as the active principle responsible for the regeneration of β-cells and normalizing all the biochemical parameters related to the patho-biochemistry of DM (Latha and Daisy, 2011). Equally, the has been reported that the antidiabetic effect potential of syringic acid may be due to the increased release of insulin from the existing β-cells and/or regenerated β-cells of the pancreas, restored insulin sensitivity or inhibition of intestinal absorption of glucose, or enhanced the utilization of glucose by peripheral tissues (Muthukumaran *et al.*, 2013). Our results are in

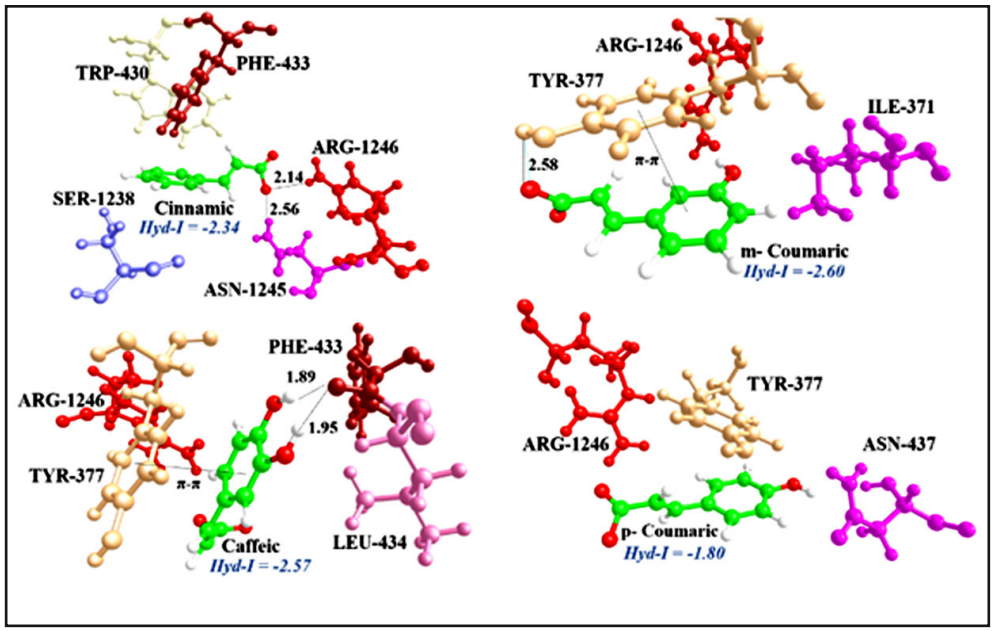

Figure 3. Interaction mode for cinnamic acid derivates in the SUR1 binding site. Hydrogen bond distances, π-π, and hydrophobic interaction are showed.

agreement with the tendencies in these references and other works, which continue to place these structures as future candidates for the treatment of DM.

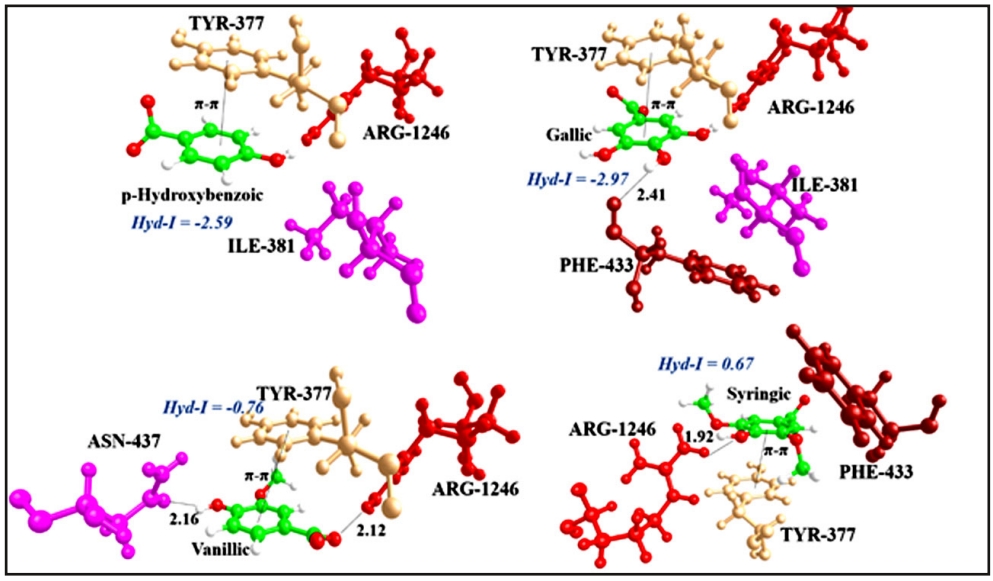

Figure 4. Interaction mode for p-hydroxybenzoic acid derivates in the SUR1 binding site. Hydrogen bond distances, π-π, and hydrophobic interaction are showed.

Chlorogenic acid showed a binding energy value of -7.6 Kcal/mol in agreement with the repaglinide. The common interaction residues remain *Arg*-1246 and *Asn*-1245, where the -OH groups substituted in the cyclohexane ring of chlorogenic acid form four hydrogen bonds (**Figure 5**). On the other hand, the -OH groups substituted in the aromatic ring also form three hydrogen bonds with *Asn*-547 residue. The similarity that repaglinide (Martinet *et al.*, 2017), chlorogenic acid partially overlaps the binding site of the glibenclamide. Therefore, competitive behavior could be expected for chlorogenic acid.

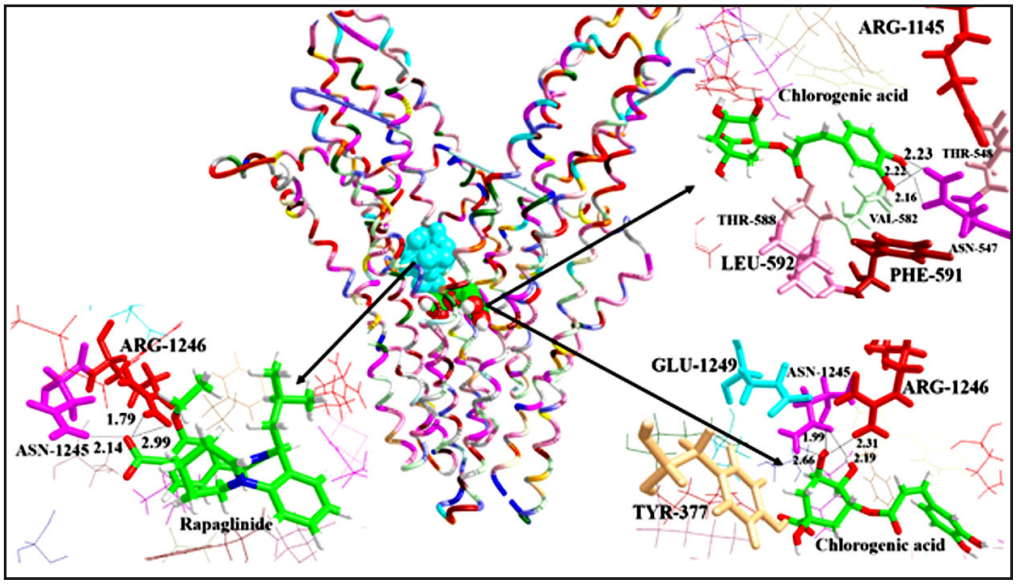

Figure 5. Interaction mode for Rapaglinide (PDB: 6JB3) and chlorogenic acid (after molecular docking) in the SUR1 binding site. Hydrogen bond (Å) and principal residues are showed.

In the past years, the potential of chlorogenic acid as a compound for the regulation of glucose metabolism has been reported (Meng *et al.*, 2013). In diabetic rats, have been reports that chlorogenic acid reduces glycemia and the glycemic index of food by attenuating the intestinal absorption of glucose (Bassoli *et al.*, 2008). Also, chlorogenic acid is involucrate in the glucose regulation via the activation of 5'-adenosine monophosphate-activated protein (AMPK) in HepG2 human hepatoma cell line (Ong *et*

al., 2013). Concerning the action as a non-sulfonylurea compound, chlorogenic acid has been reported as an insulin secretagogue increasing intracellular calcium concentrations ($([Ca^{2+}]i$) in RINm5F cells; and as an insulin sensitizer and lipid-lowering agent stimulating the expression of PPARγ and PPARα, respectively (Sánchez *et al.*, 2017). Our results are in agreement with the tendencies in these references and others' works.

Normal mode analysis

To explore the SUR1 dynamics in the presence of chlorogenic acid ligand, we have carried out a normal mode analysis (NMA), which characterizes all possible deformations that a protein can undergo around an equilibrium conformational (Brooks and Karplus, 1983; Go *et al.*, 1983). The low-frequency vibrations typically correspond to collective motions, while the higher frequency modes represent local deformations. Several studies have shown that normal modes with large fluctuations are the ones that are also functionally relevant (Mohammad *et al.*, 2018). We have used the default settings of WEBnm@ to performance an Atomic Displacement Analysis, to identify the flexible region of the SUR1, and Mode Visualization and Vector Field Analysis to obtain the direction of collective motions of the SUR1. **Figure 6** shows the normalized atomic fluctuation profile for the SUR1 in presence of repaglinide.

The peaks in an atomic fluctuation profile correspond to the relatively more flexible regions of a protein. Therefore, **Figure 6** shows some fluctuations between 1.5 Å and 1.7 Å for the interaction SUR1-ligand zone (*Tyr*-377 → *Asn*-437, green color in **Table 4**). Also, we observed fluctuations up to 2 Å near *Leu*-592 and *Val*-596.

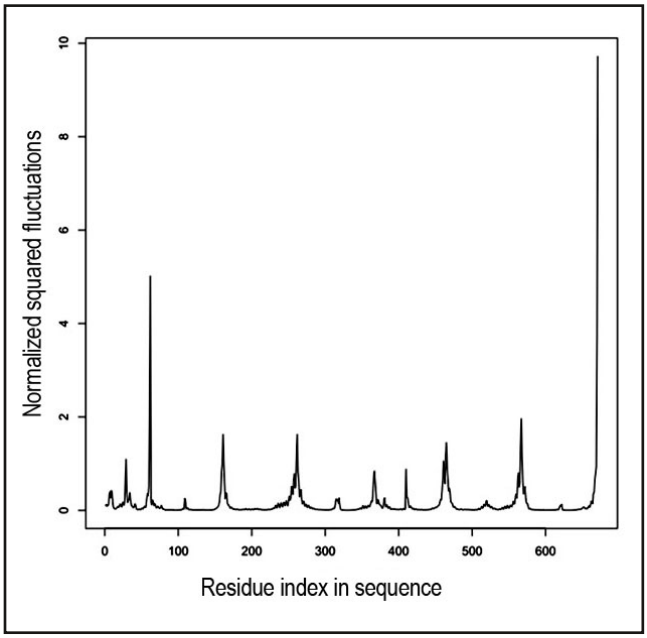

Figure 6. Fluctuation flexibility of the Cα atoms of the SUR1.

Figure 7 shows the displacement square of each C-α atom (for modes 7 to 12) normalized so that the sum of all residues is equal to 100. The highest values correspond to the most displaced regions. Clusters of peaks on the plots identify significantly displaced regions, while isolated peaks may reflect local flexibility. In agreement with the discussion of **Figure 6**, mode 9 shows a fluctuation between 1.5 Å and 2 Å for the interaction SUR1-ligand zone.

Conclusions

We report the bioavailability analysis for ten secondary metabolites with hypoglycemic activity reported, from *M. alba*. Most of the compounds showed agreement with Lipinski's "rule of 5", which reflects a good bioavailability in all of them. According to the bioactivity scores values, the secondary meta-

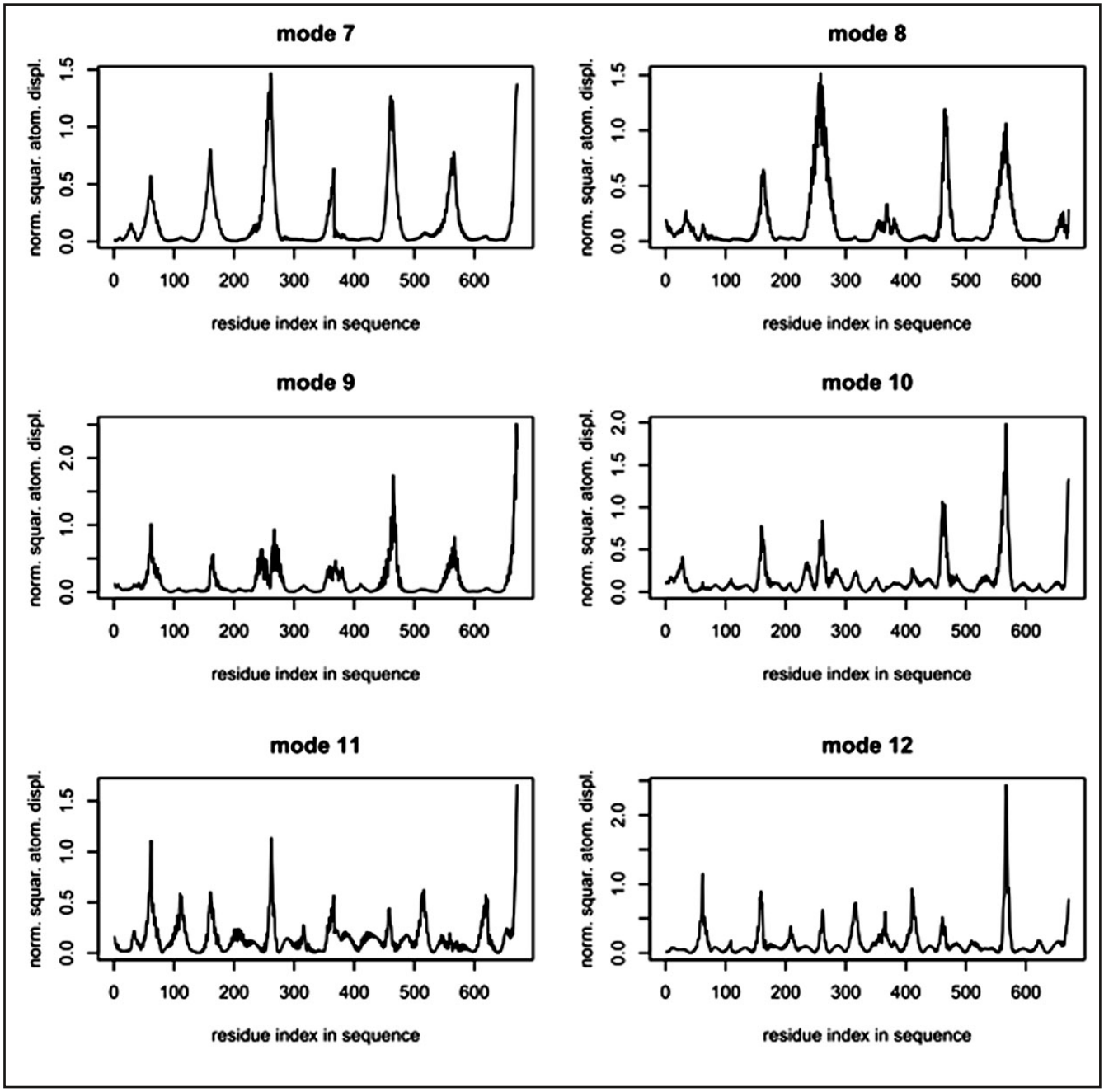

Figure 7. Displacement square of each Cα atom for modes 7 to 12.

bolites studied can act primarily as ionic channel modulators, nuclear receptor ligands, and other enzyme inhibitors. The molecular similarity was evaluated by averaging geometric parameters (3D-Shape) and electrostatic potential (ESP). The results show that the most secondary metabolites would have a similar mode of action as the neteglinide, with the average similarity between 0.72 and 0.80. This last idea is reinforced by the results for molecular docking with the repaglinide active site of SUR1, highlighting the interaction of the molecules studied with the amino acid residues: *Arg*-1246, *Tyr*-377, *Asn*-437, *Leu*-434, *Phe*-433, *Trp*-430, and *Ile*-381, with a range interaction-free energy

between -5.2 and -7.9 Kcal/mol. Chlorogenic acid showed the best performance, which reinforces experimental and theoretical studies on the anti-hypoglycemic activity of this compound. However, other secondary metabolites present in *M. alba* also showed a good performance in the interaction with the SUR1 active zone.

Acknowledgments

The authors acknowledge and thank the Universidad Nacional Experimental del Táchira, Venezuela and the Decanato de Investigación for the support of this research.

Declaration of interests

The authors declare that they have no known competing financial interests or personal relationships that could have appeared to influence the work reported in this paper.

References

Adisakwattana S. 2017. Cinnamic acid and its derivatives: mechanisms for prevention and management of diabetes and its complications. Nutrients 9(2): 163–200.

Bassoli B, Cassola P, Borba-Murad G, Constantin C, Salgueiro-Pagadigorria L, Bazotte RB, da Silva RS, de Souza HM. 2008. Chlorogenic acid reduces the plasma glucose peak in the oral glucose tolerance test: effects on hepatic glucose release and glycaemia. Cell Biochem Funct 26(3): 320–328.

Bender A, Glen RC. 2004. Molecular similarity: a key technique in molecular informatics. Org Biomol Chem 2(22):3204–3218.

Bhal SK. 2012. LogP-Making Sense of the Value. Retrieved from ACD/Labs: http://www.dlabs.com/logp

Brooks B, Karplus M. 1983. Harmonic dynamics of proteins: normal modes and fluctuations in bovine pancreatic trypsin inhibitor. Proc Natl Acad Sci USA 80(21): 6571–6577.

Chaudhury A, Duvoor C, Reddy Dendi VS, Kraleti S, Chada A, Ravilla R, Marco A, Shekhawat NS, Montales MT, Kuriakose K, Sasapu A, Beebe A, Patil N, Musham CK, Lohani GP, Mirza WL.2017. Clinical review of antidiabetic drugs: implications for type 2 diabetes mellitus management. Front Endocrinol (Lausane) 8(6): 1–12.

Daina AM, Michielin O, Zoete V. 2017. Swiss ADME: a free web tool to evaluate pharmacokinetics, drug-likeness and medicinal chemistry friendliness of small molecules. Sci Rep 7: 42717, 13 pp.

Daina A, Zoete V. 2016. A BOILED-Egg to predict gastrointestinal absorption and brain penetration of small molecules. Chem Med Chem 11(11): 1117–1121.

Ding D, Wang M, Wu JX, Kang Y, Chen L. 2019. The structural basis for the binding of repaglinide to the pancreatic KATP channel. Cell Rep 27(6): 1848–1857.

Doan K, Ko C, Kinyua A, Yang D, Choi Y, Oh I, Nguyen N, Ko A, Choi J, Jeong Y, Jung M, Cho W, Xu S, Park K, Park W, Choi S, Kim H, Moh S, Kim K. 2015. Gallic acid regulates body weight and glucose homeostasis through AMPK activation. Endocrinology 156(1): 157–168.

Eckert H, Bajorath J. 2007. Molecular similarity analysis in virtual screening: foundations, limitations and novel approaches. Drug Discov Today 12(5-6): 225–233.

Ernawati T, Mun'im A, Hanafi M, Yanuar A. 2018. In silico evaluation of molecular interactions between known α-glucosidase inhibitors and homologous α-glucosidase enzymes from *Saccharomyces cerevisiae*, *Rattus norvegicus*, and GANC-human. Thai J Pharm Sci42(1): 14–20.

Fernandes CA, Cardoso FF, Cavalcante WG, Soares AM, Dal-Pai M, Gallacci M, Fontes MR. 2015. Structural basis for the inhibition of a phospholipase a2-like toxin by caffeic and aristolochic acids. PLoS ONE 10(7): e0133370.

Furman B. 2017. Glitinides. Reference Module in Biomedical Sciences: 1–4.

Gasteiger J, Marsili M. 1980. Iterative partial equalization of orbital electronegativity a rapid access to atomic charges. Tetrahedron 36(22): 3219–3228.

Go N, Noguti T, Nishikawa T. 1983. Dynamics of a small globular protein in terms of low-frequency vibrational modes. Proc Natl Acad Sci USA 80(12): 3696–3700.

Gribble FM, Reimann F. 2003. Sulphonylurea action revisited: the post-cloning era. Diabetología 46: 875–891.

Guardado-Mendoza R, Prioletta A, Jiménez-Ceja LM, Sosale A, Folli F. 2013. The role of nateglinide and repaglinide, derivatives of meglitinide, in the treatment of type 2 diabetes mellitus. Arch Med Sci 9(5): 936–943.

Hansen AM, Christensen IT, Hansen JB, Carr RD, Ashcroft FM, Wahl P. 2002. Differential interactions of nateglinide and repaglinide on the human β-cell sulphonylurea receptor 1. Diabetes 51(9): 2789–2795.

Henquin JC. 2004. Pathways in beta-cell stimulus-secretion coupling as targets for therapeutic insulin secretagogues. Diabetes 53(suppl 3): S48–S58.

Hitchcock SA, Pennington LD. 2006. Structure–brain exposure relationships. J Med Chem 49(26): 7559–7583.

Hollup SN, Sælensminde G, Reuter N. 2005. WEBnm@: a web application for normal mode analysis of proteins. BMC Bioinformatics 6: 52, 8 pp.

Hossain MU, Khan MA, Rakib-Uz-Zaman SM, Ali MT, Islam MS, Keya CA, Salimullah M. 2016. Treating diabetes mellitus: pharmacophore based designing of potential drugs from gymnema sylvestre against insulin receptor protein. Biomed Res Int 2016: 3187647, 16 pp.

Kyriakis E, Stravodimos GA, Kantsadi AL, Chatzileontiadou DS, Skamnaki VT, Leonidas D. 2015. Natural flavonoids as antidiabetic agents. The binding of gallic and ellagic acids to glycogen phosphorylase b. FEBS Lett 589(15): 1787–1794.

Latha RC, Daisy P. 2011. Insulin-secretagogue, antihyperlipidemic and other protective effects of gallic acid isolated from *Terminalia bellerica* Roxb. in streptozotocin-induced diabetic rats. Chem Biol Interact 189(1-2): 112–118.

Lipinski C, Lombardo F, Dominy B, Feeney P. 1997. Experimental and computational approaches to estimate solubility and permeability in drug discovery and development settings. Adv Drug Deliv Rev 23(1-2): 3–25.

Marles RJ, Farnsworth NR. 1995. Antidiabetic plants and their active constituents. Phytomedicine 2(2): 137–189.

Martin GM, Yoshioka C, Rex EA, Fay JF, Xie Q, Whorton M, Chen J, Shyng S. 2017. Cryo-EM structure of the ATP-sensitive potassium channel illuminates mechanisms of assembly and gating. eLife6: e24149.

Matboli M, Eissa S, Ibrahim D, Hegazy MG, Imam SS, Habib EK 2017. Caffeic acid attenuates diabetic kidney disease via modulation of autophagy in a high-fat diet/streptozotocin-induced diabetic rat. Sci Rep 7: 2263.

Meng S, Cao J, Feng Q, Peng J, Hu Y. 2013. Roles of chlorogenic acid on regulating glucose and lipids metabolism: a review. Evid-Based Complement Altern Med 2013: 801457, 11 pp.

Mohammad SF, Ali F, Rahman MU, Muhammad A. 2018. Normal mode analysis of thermophilic cellulase FnCel5A using elastic network models. J Proteom Bioinform 11(5): 111-116.

Molinspiration. 1986. Cheminformatics on the Web. Retrieved from http://www.molinspiration.com/

Muegge I. 2003. Selection criteria for drug-like compounds. Med Res Rev 23(3): 302–321.

Muthukumaran J, Srinivasan S, Venkatesan RS, Ramachandran V, Muruganathan U. 2013. Syringic acid; a novel natural phenolic acid; normalizes hyperglycemia with special reference to glycoprotein components in experimental diabetic rats. J Acute Dis 2(4): 304–309.

Nicasio P, Aguilar L, Aranda E, Ortíz S, González M. 2005. Hypoglycemic effect and chlorogenic acid content in two *Cecropia* species. Phytother Res 19(8): 661-664.

Ochieng PJ, Sumaryada T, Okun D 2017. Molecular docking and pharmacokinetic prediction of herbal derivatives as maltase-glucoamylase inhibitor. Asian J Pharm Clin Res10(9): 392–398.

Ong K, Hsu A, Tan B. 2013. Anti-diabetic and anti

-lipidemic effects of chlorogenic acid are mediated by AMPK activation. Biochem Pharmacol 85(9): 1341–1351.

Pajouhesh H, Lenz GR. 2005. Medicinal chemical properties of successful central nervous system drugs. NeuroRx 2(4): 541–553.

Pedretti A, Villa L, Vistoli G. 2004. VEGA- an open platform to develop chemo-bio-informatics applications, using plug-in architecture and script programming. J Comput Aided Mol Des 18(3): 167–173.

Proks P, Ashcroft FM. 2009. Modeling KATP channel gating and its regulation. Prog Biophys Mol Biol 99(1): 7–19.

Vinayagam R, Jayachandran M, Xu B. 2015. Antidiabetic effects of simple phenolic acids: A comprehensive review. Phytother Res 30(2): 184–199.

Remko, M. 2009. Theoretical study of molecular structure, pKa, lipophilicity, solubility, absorption, and polar surface area of some hypoglycemic agents. Theochem 897(1-3): 73–82.

Sanchez MB, Miranda-Perez E, Verjan JC, Barrera M, Perez-Ramos J,Alarcon-Aguilar FJ. 2017. Potential of the chlorogenic acid as multitarget agent: Insulin-secretagogue and PPAR α/γ dual agonist. Biomed Pharmacother 94:169–175.

Schmidt MW, Baldridge KK, Boatz JA, Elbert ST, Gordon MS, Jensen JH, Koseki S, Matsunaga N, Nguyen KA, Su S, WindusTL, Dupuis M, Montgomery J Jr. 1993. General atomic and molecular electronic structure system. J Comput Chem 14(11): 1347–1363.

Shin WH, Zhu X, Bures M, Kihara D. 2015. Three-dimensional compound comparison methods and their application in drug discovery. Molecules 20(7): 12841–12862.

Shinkai H.2000. Novel antidiabetic agents. Expert Opin Ther Pat 10(1): 59–66.

Shukla PK, Gautam L, Sinha M, Kaur P, Sharma S, Singh TP. 2015. Structures and binding studies of the complexes of phospholipase A2 with five inhibitors. Biochim Biophys Acta 1854(4): 269–277.

Teng H, Chen L. 2017. α-Glucosidase and α-amylase inhibitors from seed oil: A review of liposoluble substance to treat diabetes. Crit Rev Food Sci Nutr 57(16):3438–3448.

Vainio MJ, Puranen JS, Johnson MS. 2009. ShaEP: molecular overlay based on shape and electrostatic potential. J Chem Inf Model 49(2): 492–502.

Veber D, Johnson S, Cheng H, Smith B, Ward K, Kopple K. 2002. Molecular properties that influence the oral bioavailability of drug candidates. J Med Chem 45(12): 2615–2623.

Wishart DS, Feunang YD, Guo AC, Lo EJ, Marcu A, Grant JR, Sajed T, Johnson D, Li C, Sayeeda Z, Assempour N, Iynkkaran I, Liu Y, Maciejewski A, Gale N, Wilson A, Chin L, Cummings R, Le D, Pon A, Knox C, Wilson M. 2017. DrugBank 5.0: a major update to the DrugBank database for 2018. Nucleic Acids Res 46(D1): D1074–D1082.

Wu JX, Ding D, Wang M, Kang K, Zeng X, Chen L. 2018. Ligand binding and conformational changes of SUR1 subunit in pancreatic ATP-sensitive potassium channels. Protein Cell 9(6): 553–567.

Yuan Q, Zhao L. 2017. The mulberry (*Morus alba* L.) fruit-a review of characteristic components and health benefits. J Agr Food Chem 65(48): 10383–10394.

Recibido: 18/09/2020
Aceptado: 01/11/2020